REPORT DOCUMENTATION PAGE

Form Approved OMB No. 0704-0188

1. REPORT DATE *(DD-MM-YYYY)*	2. REPORT TYPE	3. DATES COVERED *(From – To)*
25-01-2008	Final Report	30 September 2005 - 24-Jun-09

4. TITLE AND SUBTITLE

Research and Development of a Scaled Joined Wing Flight Vehicle

5a. CONTRACT NUMBER
FA8655-05-1-3076

5b. GRANT NUMBER

5c. PROGRAM ELEMENT NUMBER

6. AUTHOR(S)

Professor Afzal Suleman

5d. PROJECT NUMBER

5d. TASK NUMBER

5e. WORK UNIT NUMBER

7. PERFORMING ORGANIZATION NAME(S) AND ADDRESS(ES)

Instituto Superior Tecnico
Departmento de Engenharia Mecanica
Av. Rovisco Pais, 1
Lisbon 1049-001
Portugal

8. PERFORMING ORGANIZATION REPORT NUMBER

N/A

9. SPONSORING/MONITORING AGENCY NAME(S) AND ADDRESS(ES)

EOARD
Unit 4515 BOX 14
APO AE 09421

10. SPONSOR/MONITOR'S ACRONYM(S)

11. SPONSOR/MONITOR'S REPORT NUMBER(S)
Grant 05-3076

12. DISTRIBUTION/AVAILABILITY STATEMENT

Approved for public release; distribution is unlimited.

13. SUPPLEMENTARY NOTES

14. ABSTRACT

This report results from a contract tasking Instituto Superior Tecnico as follows: The Grantee will investigate the aeroelastic performance of the joined wing concept. Dr. Suleman and his research team have proposed to investigate the aeroelastic performance of the joined wing concept by analyzing, designing, manufacturing, and wind tunnel testing a aeroelastically scaled models. The first step will include designing a test assembly to conduct aeroelastic flutter and gust response tests. A fairly flexible wing with low bending and torsion mode frequencies is envisioned in order to study the aeroelastic phenomena in a low subsonic regime. The structure of the joined wing will be analyzed in order to determine its vibrational behavior. Design aspects to be considered include the spanwise loadings and the design of wing camber and twist. A comparison of experimental and computational results will be conducted. Nonlinear structural issues will also be addressed. In order to predict the post-buckling behavior of the joined-wing structure, this task will concentrate on the development of higher-order geometric nonlinearity models for the joined-wing concept. Appropriate criteria will be determined for (a) stiffness and weight effects on vehicle handling and flutter, and (b) ultimate strength and stability; (c) skin postbuckling and stringer column buckling of skin/stringer configurations, and (d) critical damage conditions associated with ultimate strength.

15. SUBJECT TERMS
EOARD, Aerodynamics, joined-wing, Aeroelasticity

16. SECURITY CLASSIFICATION OF:			17. LIMITATION OF ABSTRACT	18, NUMBER OF PAGES	19a. NAME OF RESPONSIBLE PERSON
a. REPORT	b. ABSTRACT	c. THIS PAGE			SURYA SURAMPUDI
UNCLAS	UNCLAS	UNCLAS	UL	39	19b. TELEPHONE NUMBER *(Include area code)* +44 (0)1895 616021

AEROELASTIC SCALING OF A JOINED WING SENSORCRAFT CONCEPT

Final Report

January-December 2007

and

Proposal Report

2008-2010

Principal Investigator:

Afzal Suleman, IST, Professor

USAF Collaborators:

Max Blair, AFRL, Research Scientist

Robert Canfield, AFIT, Professor

Graduate Students/Technician at IST/AFA, Portugal:

Antonio Costa (Laboratory Technician)

Jenner Richards (MASc Student)

Graduate Student at USAF/AFIT:

LtCor Vanessa Bond (USAF/AFIT PhD Student)

Summary

This document reports the work performed during Year 4 (Jan-Dec 2007) of the project in the framework of the collaborative research between Instituto Superior Tecnico and the U.S. Air Force (AFRL-WPAFB) under the Grant/Cooperative Agreement Award No. FA8655-05-1- 3076. The objective of the current research project is to develop computational and experimental models and a 5m span aeroelastically scaled RPV for flight testing and evaluating the aeroelastic behaviour of the Boeing Joined-Wing Sensorcraft. To this end, a modified aeroelastic scaling methodology is proposed that addresses the issues raised during the aeroelastic scaling procedure for the AFRL Joined-Wing model (see Report-1).

Furthermore, this report also presents the proposal for future work to be carried out between 2008-2010 and the budget details are also included.

Contents

Table of Figures

1 Introduction

This report outlines the progress made in the design of an 1/9th aeroelastically scaled remotely piloted vehicle to investigate the aeroelastic characteristics and gust response of the full scale Boeing/USAF Sensorcraft concept. The project is part of an ongoing collaboration between the AFRL-AFIT at the U.S. Air Force in Dayton OH, Instituto Superior Técnico in Lisbon and the Portuguese Air Force Academy in Sintra.

Previous work has been completed on an earlier joined-wing concept at the Instituto Superior Técnico which included the designing, building and subsequent GVT and WT testing of the proposed AFRL joined-wing concept. This effort has yielded aeroelastic scaling and design techniques that serve as the foundation for the current proposed research.

2 Objective of Work

The ultimate goal of the project is to experimentally demonstrate the viability of HALE (high-altitude long-endurance) designs with significantly reduced weight, due to reduced loads, without increased risk. In order to design effective gust-load alleviation (GLA) technologies, a better understanding of the gust response of the Joined Wing Sensorcraft is desired.

Flight testing of a scaled RPV provides a low cost and effective way to explore the aeroelastic and gust response of the joined wing configuration. In addition, it will serve to validate the scaling methods employed and support management planning for future tests of Sensorcraft technologies.

A balance is struck between fidelity of results and the overall costs. As such, a limited physics model (the small disturbance linear potential PDE) is chosen to produce a low cost, low risk model. It is believed however that this method will provide an effective means to explore the aeroelastic response and give good insight to the operability of Sensorcraft vehicles. A successfully scaled RPV will also serve as a test-bed for exploring validating gust-load alleviation (GLA) solutions, determine aero-servo elastic transfer functions and possibly investigate non-linear, aeroelastic effects.

3 Theory

The following section presents the theory to be used in the scaling of the RPV along with the assumptions that are made in order to design a low cost, effective test article.

3.1 Why Develop a Physical Scaled Model?

Due to the complexity of aeroelastic problems, especially dynamic problems such as flutter, purely analytical techniques are not exclusively relied upon in the design process. Despite recent improvements in CFD, fluid/structure interaction and constitutive models, “there is little reliance on these tools… owing to the prevailing lack of confidence in quantitative estimates of loads and response” (1). A properly designed model will display the same aeroelastic behaviors as the full scale aircraft, with the flutter/divergence velocity and frequencies varying by known scale factors (2).

In order to map the aeroelastic properties of the full scale aircraft to the scaled model, valid scaling factors must be used. These scaling factors are derived from non-dimensional parameters that appear in the equations that govern the aerodynamics, the structure and their coupling. These scaling

parameters are subject to constraints posed by the wind-tunnel or environment in which the model will operate.

3.2 Aeroelastic Scaling

Due to the complex nature of the problem, and the limited time and resources, some assumptions are applied to simplify the scaling process. In the present case, the aerodynamic scaling procedure will be governed by the small disturbance, linear potential partial differential equations (PDE). These limited physics are adequate for a low-cost exploration of flight mechanics, of an aeroelastically scaled joined-wing Sensorcraft, in gust conditions.

When the equations of motion describing this system are non-dimensionalized, they yield a set of parameters that are used for scaling the baseline aircraft.

3.3 Aeroelastic Equations of Motion (EOM)

If structural damping is ignored, the governing aeroelastic equations, in physical space **y,** are as follows.

$$\boldsymbol{M}\ddot{\underline{y}} + \boldsymbol{K}\underline{y} = q\boldsymbol{Q}\underline{y} \tag{1}$$

$$or \begin{Bmatrix} \boldsymbol{F} \\ \boldsymbol{M} \end{Bmatrix}_I + \begin{Bmatrix} \boldsymbol{F} \\ \boldsymbol{M} \end{Bmatrix}_s = q\boldsymbol{Q}\underline{\boldsymbol{y}} \tag{2}$$

If the above equation is written in a reduced form representing two degrees of freedom, translations and rotations, it becomes

$$\begin{bmatrix} \boldsymbol{M}_{11} & \boldsymbol{M}_{12} \\ \boldsymbol{M}_{21} & \boldsymbol{M}_{22} \end{bmatrix} \begin{Bmatrix} \ddot{\boldsymbol{X}} \\ \ddot{\boldsymbol{\theta}} \end{Bmatrix} + \begin{bmatrix} \boldsymbol{K}_{11} & \boldsymbol{K}_{12} \\ \boldsymbol{K}_{21} & \boldsymbol{K}_{22} \end{bmatrix} \begin{Bmatrix} \boldsymbol{X} \\ \boldsymbol{\theta} \end{Bmatrix} = \frac{\rho \boldsymbol{V}^2}{2} \begin{bmatrix} \boldsymbol{b}^2 & \boldsymbol{0} \\ \boldsymbol{0} & \boldsymbol{b}^3 \end{bmatrix} \begin{bmatrix} \boldsymbol{Q}_{11} & \boldsymbol{Q}_{12} \\ \boldsymbol{Q}_{21} & \boldsymbol{Q}_{22} \end{bmatrix} \begin{Bmatrix} \boldsymbol{X} \\ \boldsymbol{\theta} \end{Bmatrix} \tag{3}$$

Where

$\boldsymbol{X}$	Vector of translational degrees of freedom
	Vector of rotational degrees of freedom
$\boldsymbol{M}_{ij}$	Block matrix terms in mass/inertia matrix
$\boldsymbol{K}_{ij}$	Block matrix terms in stiffness matrix
$\boldsymbol{b}$	Reference length
$\boldsymbol{Q}_{ij}$	Block matrix aerodynamic terms

If this equation is then written in terms of the fundamental, or primary, quantities of mass, length and time (**M**, **L** and **T**) then we get the following

$$\begin{bmatrix} \boldsymbol{M} & \boldsymbol{ML} \\ \boldsymbol{ML} & \boldsymbol{ML}^2 \end{bmatrix} \begin{Bmatrix} \boldsymbol{LT}^{-2} \\ \boldsymbol{T}^{-2} \end{Bmatrix} + \begin{bmatrix} \boldsymbol{MT}^{-2} & \boldsymbol{MLT}^{-2} \\ \boldsymbol{MLT}^{-2} & \boldsymbol{ML}^{-2}\boldsymbol{T}^{-2} \end{bmatrix} \begin{Bmatrix} \boldsymbol{L} \\ \boldsymbol{nd} \end{Bmatrix} = \boldsymbol{ML}^{-1}\boldsymbol{T}^{-2} \begin{bmatrix} \boldsymbol{L}^2 & \boldsymbol{0} \\ \boldsymbol{0} & \boldsymbol{L}^3 \end{bmatrix} \begin{bmatrix} \boldsymbol{L}^{-1} & \boldsymbol{nd} \\ \boldsymbol{L}^{-1} & \boldsymbol{nd} \end{bmatrix} \begin{Bmatrix} \boldsymbol{L} \\ \boldsymbol{nd} \end{Bmatrix} \tag{4}$$

The above is a “complete” equation and contains only primary quantities of mass, length and time (**M**, **L** and **T**). We can choose any three base units of measurement that are independent products of M, L and T to serve as the basis of our scaling method, and thereby non-dimensionalize the EOM. Several combinations are possible but for the present case we will use length, density and velocity

(where density and velocity are referred to as surrogate parameters, as they are combinations of the primary quantities). These particular quantities are chosen so as to allow us to choose the model size, flight test altitude (limited by visual range of remote pilot) and the velocity.

3.3.1 Non-Dimensionalization of Primary Quantities (M, L and T)

Having chosen three convenient base units for the dynamic analysis, we can now use them to write the primary quantities in non-dimensional form. We start with the base unit of length and define a non-dimensional coordinate system (ζ, ϕ), such that

$$\boldsymbol{x = b\zeta} \quad \boldsymbol{and} \quad \boldsymbol{\theta = \phi} \tag{5}$$

Non-dimensional time (τ) is derived using the velocity and the geometric scaling factor. Its derivatives are found by use of the chain rule with the results shown below.

$$\tau = \frac{tV}{b} \tag{6}$$

$$\dot{x} = V\zeta' \quad \ddot{x} = \frac{V^2}{b}\zeta'' \qquad \theta = \frac{V}{b}\phi' \quad \ddot{\theta} = \frac{V^2}{b^2}\ddot{\phi} \tag{7}$$

Finally, we can write the mass in non-dimensional form ($\bar{M}$) using the density and the length scale factor to yield the following relationships.

$$M_{11} = \rho b^3 \bar{M}_{11} \qquad M_{12} = M_{21} = \rho b^4 \bar{M}_{12} \qquad M_{11} = \rho b^5 \bar{M}_{22} \tag{8}$$

3.3.2 EOM's in Dimensionless Form

With the primary quantities in dimensionless form, we can now rewrite the aeroelastic equations of motion in a non-dimensional form. Starting with the inertial force and moment terms, **F** and **M** respectively,

$$\begin{Bmatrix} F \\ M \end{Bmatrix}_I = \begin{bmatrix} M_{11} & M_{12} \\ M_{21} & M_{22} \end{bmatrix} \begin{Bmatrix} \ddot{X} \\ \ddot{\theta} \end{Bmatrix} = \begin{bmatrix} \rho b^3 \bar{M}_{11} & \rho b^4 \bar{M}_{12} \\ \rho b^4 \bar{M}_{21} & \rho b^5 \bar{M}_{22} \end{bmatrix} \begin{Bmatrix} \frac{V^2}{b}\zeta'' \\ \frac{V^2}{b^2}\phi'' \end{Bmatrix} \tag{9}$$

$$\begin{Bmatrix} F \\ M \end{Bmatrix}_I = \begin{bmatrix} \rho V^2 b^2 M_{11} & \rho V^2 b^2 M_{12} \\ \rho V^2 b^3 \bar{M}_{21} & \rho V^2 b^3 \bar{M}_{22} \end{bmatrix} \begin{Bmatrix} \zeta'' \\ \phi'' \end{Bmatrix} = \begin{bmatrix} \rho V^2 b^2 & 0 \\ 0 & \rho V^2 b^3 \end{bmatrix} \begin{bmatrix} M_{11} & M_{12} \\ \bar{M}_{21} & \bar{M}_{22} \end{bmatrix} \begin{Bmatrix} \zeta'' \\ \phi'' \end{Bmatrix} \tag{10}$$

$$\therefore \begin{Bmatrix} F \\ M \end{Bmatrix}_I = \begin{bmatrix} \rho V^2 b^2 & 0 \\ 0 & \rho V^2 b^3 \end{bmatrix} \begin{Bmatrix} \bar{F} \\ \bar{M} \end{Bmatrix}_I \tag{11}$$

$$or \begin{Bmatrix} \bar{F} \\ \bar{M} \end{Bmatrix}_I = \begin{bmatrix} \frac{1}{\rho V^2 b^2} & 0 \\ 0 & \frac{1}{\rho V^2 b^3} \end{bmatrix} \begin{Bmatrix} F \\ M \end{Bmatrix}_I \tag{12}$$

The same procedure can be used to derive the forces and moments due to the stiffness terms. Defining the non-dimensional stiffness terms as

$$K_{11} = \rho b V^2 \bar{K}_{11} \qquad K_{12} = K_{21} = \rho b^2 V^2 \bar{K}_{11} \qquad K_{22} = \rho b^3 V^2 \bar{K}_{22} \tag{13}$$

Repeating the similar procedure followed for the inertial terms yields the following

$$\begin{Bmatrix} F \\ M \end{Bmatrix}_s = \begin{bmatrix} \rho V^2 b^2 & 0 \\ 0 & \rho V^2 b^3 \end{bmatrix} \begin{Bmatrix} \bar{F} \\ \bar{M} \end{Bmatrix}_s \tag{14}$$

$$or \begin{Bmatrix} \bar{F} \\ \bar{M} \end{Bmatrix}_s = \begin{bmatrix} \frac{1}{\rho V^2 b^2} & 0 \\ 0 & \frac{1}{\rho V^2 b^3} \end{bmatrix} \begin{Bmatrix} F \\ M \end{Bmatrix}_s \tag{15}$$

Finally, introducing the scaling factors from (8) and (13) into equation (1) and pre-multiplying by

$$\begin{bmatrix} \frac{1}{\rho V^2 b^2} & 0 \\ 0 & \frac{1}{\rho V^2 b^3} \end{bmatrix} \tag{16}$$

Yields the aeroelastic equations in non dimensional form

$$\begin{bmatrix} \bar{M}_{11} & \bar{M}_{12} \\ \bar{M}_{21} & \bar{M}_{22} \end{bmatrix} \begin{Bmatrix} \zeta'' \\ \phi'' \end{Bmatrix} + \begin{bmatrix} \bar{K}_{11} & \bar{K}_{12} \\ \bar{K}_{21} & \bar{K}_{22} \end{bmatrix} \begin{Bmatrix} \zeta \\ \phi \end{Bmatrix} = \begin{bmatrix} 1/2 & 0 \\ 0 & 1/2 \end{bmatrix} \begin{bmatrix} bQ_{11} & Q_{12} \\ bQ_{21} & Q_{22} \end{bmatrix} \begin{Bmatrix} \zeta \\ \phi \end{Bmatrix} \tag{17}$$

It should be noted that the zero frequency (i.e. steady-state) response for any number of trimmed aerodynamic attitudes can be described if the inertial terms in the above equations are omitted

$$\begin{bmatrix} \bar{K}_{11} & \bar{K}_{12} \\ \bar{K}_{21} & \bar{K}_{22} \end{bmatrix} \begin{Bmatrix} \zeta \\ \phi \end{Bmatrix} = \begin{bmatrix} 1/2 & 0 \\ 0 & 1/2 \end{bmatrix} \begin{bmatrix} bQ_{11} & Q_{12} \\ bQ_{21} & Q_{22} \end{bmatrix} \begin{Bmatrix} \zeta \\ \phi \end{Bmatrix} \tag{18}$$

3.3.3 Simplification Using Modal Transformation

Equation (17) above consists of *m* equations, where *m* is the number of degrees of freedom (DOF)used to describe the system. If the number of DOFs is large, the resulting coupled equations can be very computationally intensive to solve. To reduce the order of the system, modal transformation can be used to uncouple the EOMs.

The first step is to transform from the physically meaningful coordinates of $\boldsymbol{\zeta}$ and $\boldsymbol{\varphi}$ to a new set of generalized modal coordinates, $\ddot{\hat{\boldsymbol{\zeta}}}$ and $\ddot{\hat{\boldsymbol{\phi}}}$

$$\begin{Bmatrix} \boldsymbol{\zeta} \\ \boldsymbol{\phi} \end{Bmatrix} = \boldsymbol{\psi} \begin{Bmatrix} \hat{\boldsymbol{\zeta}} \\ \hat{\boldsymbol{\phi}} \end{Bmatrix} \tag{19}$$

$\boldsymbol{\psi}$ represents the rectangular, *m x n* matrix where *n* is a number of lower order modes chosen for consideration (usually *n x m*). Substituting this new coordinate system into equation 17, after pre-multiplying by $\boldsymbol{\psi^T}$, results in a reduced system of order n

$$\begin{bmatrix} \hat{\boldsymbol{M}}_{11} & \mathbf{0} \\ \mathbf{0} & \hat{\boldsymbol{M}}_{22} \end{bmatrix} \begin{Bmatrix} \hat{\zeta}'' \\ \hat{\phi}'' \end{Bmatrix} + \begin{bmatrix} \hat{\boldsymbol{K}}_{11} & \mathbf{0} \\ \mathbf{0} & \hat{\boldsymbol{K}}_{22} \end{bmatrix} \begin{Bmatrix} \hat{\boldsymbol{\zeta}} \\ \hat{\boldsymbol{\phi}} \end{Bmatrix} = \boldsymbol{\psi}^T \begin{bmatrix} 1/2 & \mathbf{0} \\ \mathbf{0} & 1/2 \end{bmatrix} \begin{bmatrix} b\boldsymbol{Q}_{11} & \boldsymbol{Q}_{12} \\ b\boldsymbol{Q}_{21} & \boldsymbol{Q}_{22} \end{bmatrix} \boldsymbol{\psi} \begin{Bmatrix} \hat{\boldsymbol{\zeta}} \\ \hat{\boldsymbol{\phi}} \end{Bmatrix} \tag{20}$$

The above equations are non-dimensional with $\hat{\boldsymbol{M}}$ and $\hat{\boldsymbol{K}}$ being diagonal matrices representing inertia and stiffness respectively. It should be noted that the supplied modal data for the Sensorcraft data is given in terms of mass normalized modes. The following relationship between the true scaled mode shapes, $\boldsymbol{\psi}$, and the supplied mass normalized modes, $\boldsymbol{\Phi}$, is as follows

$$\boldsymbol{\Phi} = \boldsymbol{\psi} \hat{\boldsymbol{M}}^{1/2} \tag{21}$$

3.4 Scaling Parameters

In order for aeroelastic similarity to exist between an aircraft and its scaled counterpart, the non-dimensional terms that govern the aerodynamics, the structure and their coupling must be matched. These parameters appear in the EOM derived earlier (equation 17), where the non-dimensional mass/stiffness matrices and aerodynamic influence coefficients appear. It is these parameters, along with the primary quantities of **b**, **ρ** and **V** that dictate the scaling procedure. The following section will summarize both the scaling parameters and the dimensionless quantities that must be matched.

3.4.1 Primary Scaling Parameters

As was discussed earlier, the primary quantities of **b**, **ρ** and **V** were chosen as the scaling parameters based on the conditions imposed by testing a reduced scale RPV. These parameters are scaled as follows (where the subscripts r and f represent reduced and full scale respectively)

$$b_r = n_g b_f \tag{22}$$

$$V_r = n_v V_f \tag{23}$$

$$\rho_r = n_\rho \rho_f \tag{24}$$

These primary scaling quantities are the only parameters which the designer has the option to change. All of the following parameters are dictated by the choice of the primary scaling factors **b**, **ρ** and **V** and serve as necessary constraints on the model. These derived parameters need to be matched in order to ensure similarity between full and reduced scale aircraft.

3.4.2 Aerodynamic Parameters

Equation (17) dictates that the scaled aerodynamic terms be maintained. This requires that the scaled and full sized aircraft must be geometrically similar at their surface, which includes the statically deformed state. Therefore, while performing scaled flight testing, the RPV must be trimmed at the same attitude as the full scale aircraft.

The choice of scaling, based on the linear PDE equations, allows the elimination of several constraints that would be present if a more complex scaling procedure was chosen (ie one based on the Navier Stokes equations). For instance, the equations are based on thin airfoil theory which allows an arbitrary airfoil thickness to be assigned assuming the mean camber line is maintained. Also, if inviscid incompressible flow is assumed, the EOM will not constrain the Mach or Reynolds number.

Although the EOMs do not specifically require the matching of these other parameters, they are associated with real and well known phenomenon that the model may be subject to. As a result, attention should be paid to try and preserve these dimensionless quantities where possible. The following is a brief discussion of some of these other parameters and their effect on the physics of the model.

Reynolds Number - The task of matching the Reynolds number at a desired velocity/altitude is a difficult one. It requires that the viscosity of the surrounding medium be changed, which in most cases is not easily accomplished. Although it may be possible in some cryogenic wind tunnels, or through the use of different gasses, it will not be possible in situations where the test vehicle is flown in standard atmosphere. For this reason the matching of the Reynolds number will likely not be satisfied with the Sensorcraft RPV. Although this may seem of concern, “Experience has shown that it is generally of minor importance as far as aeroelastic effects for main lifting surfaces are concerned” (6). Where the Reynolds number does come into play is in the case of boundary layer effects (ie laminar flow separation). In order to eliminate these unwanted effects, special care is required in the model’s design. One possible solution could be that addition of “trip strips” or other forms of turbulators to ensure turbulent flow over the model without laminar separation. Another solution to this problem is to investigate an alternate flight condition that would be more closely matched.

Froude Number - The equilibrium equations require that the Froude number be maintained. The Froude number is a ratio between inertial and gravitational forces and in turn determines the ratio of deflections due to gravity compared to those due to aerodynamic loads. In many cases, the deflection due to gravity can be assumed insignificant compared to aerodynamic forces. If this assumption is valid the Froude number can be ignored (often the case in wind-tunnel models). However, in the case

of the unconstrained model in free flight, the Froude number may play a more significant role. In order to maintain a similitude of Froude number, the following ratio must be maintained

$$\left(\frac{\boldsymbol{V}}{\sqrt{bg}}\right)_r = \left(\frac{\boldsymbol{V}}{\sqrt{bg}}\right)_f \tag{25}$$

It should be noted that the gravitational term can be assumed to be constant and ignored in the above relationship.

3.4.3 Mass Parameters

Equation 17 shows that a similar dimensionless mass **distribution** is required. This not only includes the overall mass and moments of inertia, but also accounts for their distribution throughout the model. Although the overall mass and rotational inertia are not sufficient for matching mass distribution, it is useful to know factors that can be used to scale their values (for instance, a dynamic stability analysis of the RPV only requires the scaled mass and moments of inertia and does not depend on the distribution). The parameters that impose the constraints on the scaled models overall mass and moments of inertia are

$$M_r = \left(\frac{b_r}{b_f}\right)^3 \left(\frac{\rho_r}{\rho_f}\right) M_s = n_g^3 n_\rho M_s \tag{26}$$

$$\boldsymbol{I}_r = \left(\frac{b_r}{b_f}\right)^5 \left(\frac{\rho_r}{\rho_f}\right) \boldsymbol{I}_s = n_g^5 n_\rho \boldsymbol{I}_s \tag{27}$$

3.4.4 Stiffness Parameters

As can be seen in the governing EOM, the overall dimensionless stiffness must be matched. A stiffness scaling parameter, K, can be defined in terms of the primary quantities and is as follows

$$K_r = \left(\frac{\rho_r}{\rho_s}\right)\left(\frac{V_r}{V_s}\right)^2 \left(\frac{b_r}{b_s}\right) K_s = n_\rho n_v^2 n_g K_s \tag{28}$$

However, the above parameter has little meaning as it represents an overall stiffness and does not reflect the requirement that the distribution of stiffness throughout the model is matched.

3.4.5 Frequency Parameters

The frequency can be non-dimensionalized using the primary quantities chosen earlier

$$\bar{\omega} = \frac{\omega b}{V} \tag{29}$$

This can be used to yield the following scaling factor for converting the frequency between model and full scale values

$$\omega_r = \left(\frac{V_r}{V_s}\right)\left(\frac{b_s}{b_r}\right)\omega_s = \frac{n_g}{n_s}\omega_s \tag{30}$$

This scaling factor can be applied to either natural frequencies or the frequency associated with the aeroelastic response of the system. Since a velocity term appears in the denominator, a frequency cannot be scaled for a zero velocity condition.

The natural frequencies of the system can be interpreted as the modal solution to the full aeroelastic EOM for a zero velocity condition (ie aerodynamic terms are ignored). Unfortunately, the scaling of frequencies is then meaningless for the reason discussed previously. This might lead one to think that the natural frequencies are then invalid for use in the optimization process. However, natural frequencies are not a result of the solution to the aerolatic EOM, but rather that of the homogeneous solution to the elastic equations. As a result, their use in optimizing the mass and stiffness distributions using the modal response is allowed.

With all of the scaling parameters defined, aeroelastic similitude can be achieved. While these scaling parameters may be easy to apply directly in cases such as model geometry and velocity, they may not be so in certain other cases. For example, in the case of the present project, the stiffness and mass distributions are not know explicitly so other methods must be employed to scale these characteristics.

3.4.6 Summary

For completeness, a full list of the derived scaling parameters is presented here. They are summarized in Table 1 below.

Table 1 - Summary of Scaling Parameters

Denomination	Scale Factor	Reference Quantity
Length Scale*	$n_g = b_r/b_f$	b – wing stagger
Velocity-Ratio*	$n_v = V_r/V_f$	V – free stream velocity
Air Density Ratio*	$n_\rho = \rho_r/\rho_f$	ρ – air density
Stiffness-Ratio#	$K_r/K_s = n_\rho n_v^2 n_g$	
Frequency-Ratio#	$\omega_r/\omega_s = \frac{n_g}{n_s}$	
Mass-Ratio#	$M_r/M_s = n_g^3 n_\rho$	M – aircraft mass

* Primary quantities, # Surrogate, or dependant factors

3.5 Model Design

One design approach for developing accurate mass and stiffness distributions is to scale down the exact geometry of the full scale aircraft. Unfortunately, this is not practical in the case of the Sensorcraft for several reasons. For one, the internal structure is not given. In addition, manufacture of scaled components may be very expensive and in some cases impossible due to their small resulting sizes.

This then requires an alternative method for matching the models mass and stiffness distribution to that of the full scaled aircraft. The mass/stiffness distributions are not supplied directly to define the structural properties of the Sensorcraft. However, mass normalized modal shapes and natural frequencies of the aircraft are given.

From the governing linear elasticity equations it can be shown that any model with the same scaled mass and stiffness distribution, over the same scaled geometry, will result in the same modal shapes and frequencies as those of the full sized aircraft (after appropriate scaling). By designing a model with similar displacements under the same scaled loads, and matching mode shapes and frequencies, similarity of the mass/stiffness distributions will be achieved independent of internal structure. This then allows a simplified internal structure to be employed. The requirements of the structure are to allow a proper stiffness distribution while still fitting into available space, as well as not using up too much of the available mass. Once this is achieved, concentrated masses can be added to attain the desired mass distribution. An alternate option to adding concentrated masses is to alter the geometry of the structure such that it affects the mass without altering the stiffness. (An example of changing mass distribution without affecting the spanwise stiffness distribution would be to change the thickness of the ribs in a standard spar/rib configuration).

3.6 Aeroelastic Optimization Using Physical Parameter Update Methods

In reference (2), the author discusses at length the advantages of using a physical parameter based optimization over methods that are limited to modifying elements of the system matrices. (That is to say updating physical model properties, such as spar height or thickness, rather than the elements of the mass and stiffness matrices directly). Using physical parameter update methods require only that the structure can be represented as a finite element model. The parameters of this model can then be used as design variables in an optimization routine. The problem may be subject to constraints such as maximum stress. The model is then optimized by adjusting the design variables to minimize an objective function.

The method proposed here requires the completion of two separate optimizations. The first one seeks to match stiffness characteristics by minimizing an objective function based on error in calculated displacements of the model and scaled values obtained from the full scale aircraft. Any arbitrary load could be used, but using a representative aerodynamic load case may result in a better overall result. Aerodynamic loads produced during a stability analysis could be used to produce a set of loads for several trimmed states.

The second optimization is required to obtain the required mass distribution. This method will seek to match several actual modal shapes, of the stiffness corrected model, in order to correctly distribute the mass.

4 Review of Aeroelastic Scaling Work to Date

An extensive account of results obtained in the scaling and analysis of the previous concept can be found in references (7) and (3). As such, this section will serve to outline lessons learned from this previous work, some issues raised in reviewing this work and finally some additional methods that may warrant consideration.

4.1 Detailed Methodology

Section 3.6 described a methodology for scaling an aircraft using optimization techniques. The previous work followed this methodology closely with only a few exceptions. This section will briefly highlight some of the particular details of the previous work including any variations from the methods described earlier.

A baseline model was selected with a conventional dual spar/rib layout. Several manual design iterations were performed to determine the material properties of the individual components and then the rib thicknesses were set as design parameters. This would allow the overall mass and its distribution along the span to be modified through an optimization.

The overall optimization process involved matching the scaled mass and the first seven natural frequencies. Our hypothesis is that matching the aeroelastic response was not required if the wing were made equivalent in terms of the dynamic response. A final comparison of the optimized model and the scaled aeroelastic response is performed outside the loop[1]. If the model does not match the predicted response within the required tolerance then the baseline model is redefined and the process repeated. (This was the case here where it actually took three structural models made of different materials to yield final results).

Figure 1 below illustrates the scaling method and shows the outer loop in which the optimized structure is compared to the scaled response of the full vehicle. This method is in contrast to the preferred method of using the aeroelastic baseline within the loop. This would require performing a ZAERO analysis within the optimization loop in order to match the flutter response rather than the dynamic structural response. This method however would be very expensive computationally and was felt to be unrealistic using the current method and computational resources.

[1] *This expected aeroelastic response is scaled from a ZAERO analysis. Although the mass and stiffness matrices are not known explicitly, the aeroelastic response can be calculated using the given mass normalized matrices*

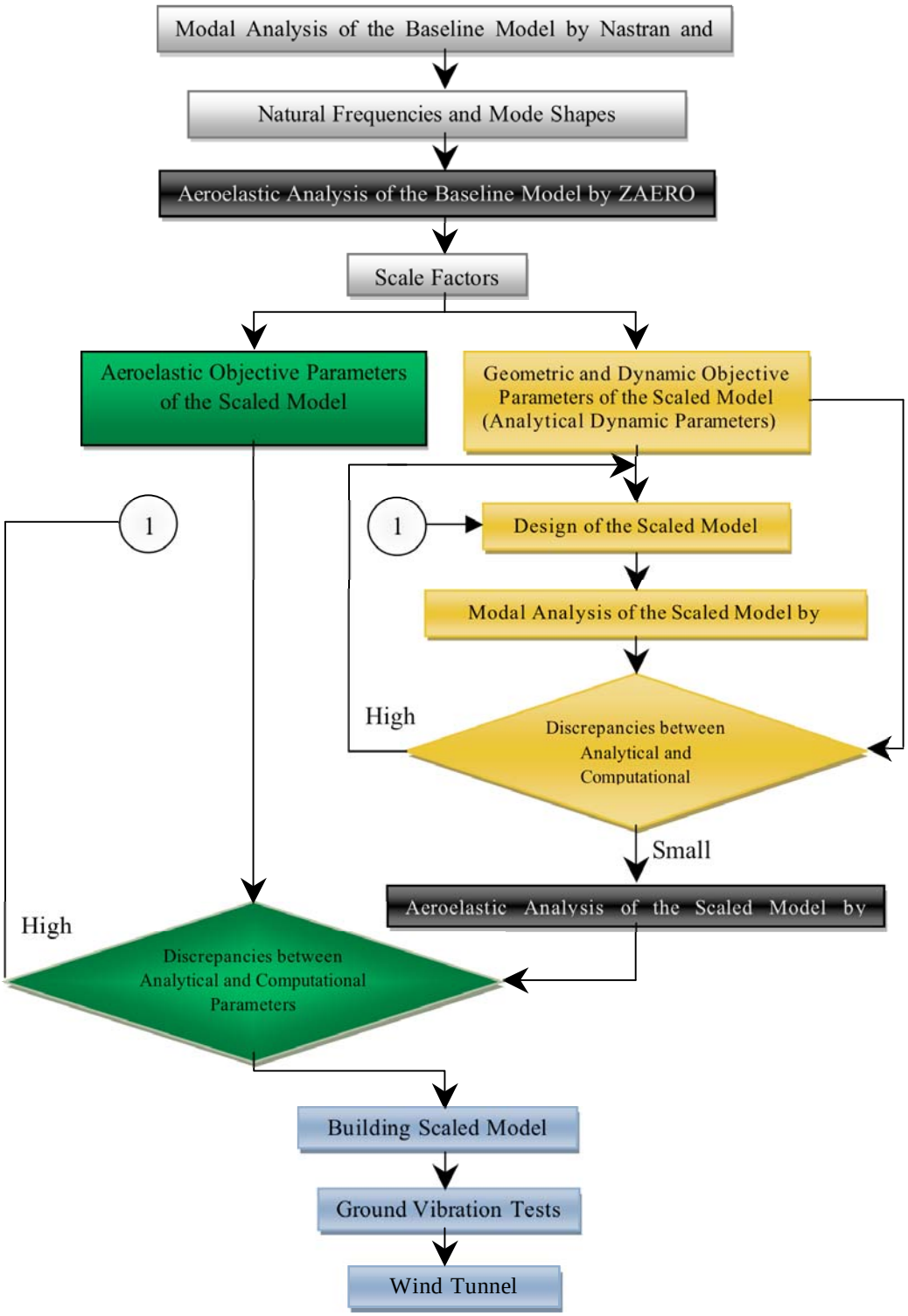

Figure 1 - Hierarchy of Scaling Methodology

4.2 Results

Please refer to the report on the completed work for the AFRL joined-sing configuration (Report1-AFRL-JoinedWing-FINAL.doc).

4.3 Possible Issues/Shortcomings

In summary, the discrepancies between baseline and scaled wing model are small in terms of flutter speed, but higher in terms of flutter frequency. Although this model predicted the aeroelastic response at the flutter speed it did not show very good agreement at other points throughout the flutter envelope.

Naturally, a reflection on the advantages and possible shortcomings of this work is necessary before continuing on to the latest configuration. The following discussion raises a few possible issues in the previous work that will be addressed in the next iteration of the project.

4.3.1 Issue 1 - Matching of stiffness and Mass Distributions

As stated earlier, by designing a model with similar displacements under the same scaled loads and matching mode shapes, similarity of the mass/stiffness distributions will be achieved independent of internal structure. However, in the previous analysis only the total scaled mass and natural frequencies were matched.

The hope here was that matching the natural frequencies of a model (while constraining the mass), will result in correct aeroelastic properties. The concern with this assumption is that a solution space of modal responses may exist for a given mass and set of modal frequencies (rather than one unique solution). If a particular aeroelastic response is required, then a unique modal response (including both frequencies and modal shapes) must be achieved.

The desired stiffness and/or mass distribution may not be accurately matched in the previous work. Normally a method such as matching the scaled displacements for an arbitrary load would tailor the stiffness distribution specifically. Then an optimization of the mass distribution would be performed based on the modal response.

4.3.2 Issue 2 – Overly Constrained Model

It is possible that the present model is overly constrained in terms of optimizing the spanwise stiffness distribution. Here the only design variable used was either the material property of the two spars or the overall thickness of the shell elements representing the spar. Altering these parameters would only serve to scale the spanwise stiffness distribution by a constant, rather than changing the stiffness distribution completely. The addition or thickening of the ribs will not serve to affect the area moment of inertia along the span (especially if considered as shell elements in the analysis) and would only serve to change the mass distribution and torsional stiffness. Even here the effects of mass distribution and torsional stiffness are totally coupled and changing their effects independently is not possible.

A proceeding section will address these concerns by posing several other model configurations being considered.

4.3.3 Issue 3 – Does Similarity Of Dynamic Response Guarantee Similar A.E. Response?

The previous analysis assumes that matching the dynamic response of the full sized aircraft will, in turn, produce a model with a similar aeroelastic response. This is of prime importance where the

optimization process is concerned since matching the dynamic response is relatively simple. This can be performed in one software package and is easily achievable in terms of present computing resources. Including the aeroelastic response in the optimization would require coupling the FEA and optimization software to the aerodynamic solvers. In addition, using first order optimization techniques for a problem with so many design parameters would require a large amount of cpu time.

Issues have been raised as to whether the assumption of matching only the dynamic response is valid. The argument for the matching of the dynamic response is this…

> *Let's assume that only one unique stiffness and mass distribution will result in the desired mode shapes and frequencies. Let's also assume that we can exclude the effects of structural damping since it is not considered in the aeroelastic calculations, even if ZAERO were included in the optimization. Now, what other property is considered in the aeroelastic calculations that could cause two dynamically equivalent wings to display different flutter responses at non-zero velocities? In other words, if the aeroelastic model only considers mass/stiffness distributions and the aerodynamic envelope why would this approach not be valid?*

It is hoped that upon completing the new model, the results may serve as a means to evaluate this assumption. Results of the previous work showed close agreement on the flutter speeds but the overall aeroelastic results did not agree with expected results. This is likely due to the other issues being addressed in this section rather than the validity of this assumption itself.

4.4 Possible Proposed Solutions

The following section contains several proposed solutions that can be applied if any of the aforementioned issues are deemed to be critical.

4.4.1 Issue 1 - Matching of Stiffness and Mass Distributions

A better method for optimizing the model may be applied to following studies. For instance, if the displacement field of the full sized aircraft subjected to a known load were supplied, an optimization could be performed to match this response. An interior penalty function could be used to minimize the error between displacements at given set of nodes for instance. A similar objective function could then be used in order to match several scaled modal shapes.

4.4.2 Issue 2 – Overly Constrained Model

In order to better match the stiffness and mass distributions, several alternate configurations are being considered. The following are a few candidate designs that may improve the results obtained from the optimization process. Please note that the pictures reflect a conventional wing design for simplicity sake, but are intended to be used for the present project. Also, some configurations are better suited for wings where the assumed stiffness function is of only one variable (ie only changes along the span) where as others account for fore and aft stiffness distribution. Due to the high aspect ratio of the Sensorcraft's wings, the single variable assumption may be valid but more investigation may be required to validate this.

Spar/Rib – often the properties of a wing can be closely duplicated using the assumption that the elastic properties are a function of one variable (torsion and bending about a locus of elastic centers, as a function of span). This is often the case in wings with a moderate to large aspect ratio and where spanwise stations can be assumed to experience no deflection other than a linear deflection and

twisting about the elastic axis. In this case the spars stiffness characteristics can be optimized and then the mass distribution tuned by the addition of concentrated masses or by varying the thickness of the spars.

If skin stiffness is a concern, the aerodynamic sleeve can be constructed in sections so that as to minimize the amount of bending/torsional stiffness contributed. Alternatively, the airfoil thickness can be reduced (recall this is allowed by the thin airfoil assumption made in the scaling process) and thereby reduce the bending stiffness.

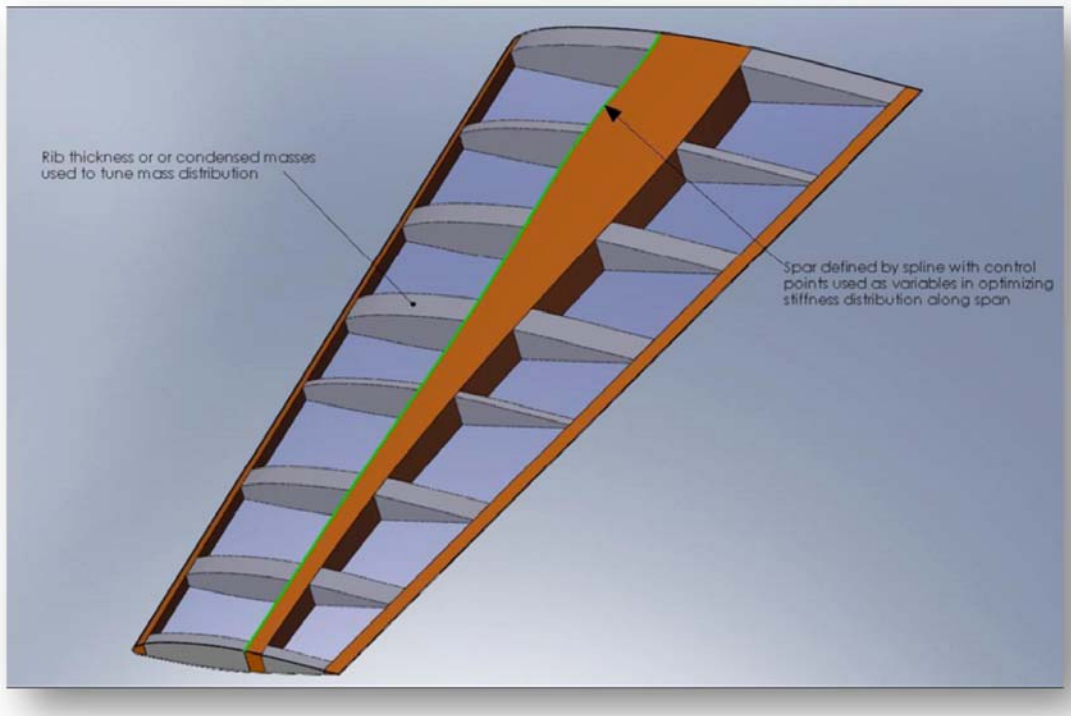

Figure 2 - Spar/Rib Configuration

In Figure 2 above, a structure is pictured with the spar's profile described by a spline. The control points of this spline would be used as the variables for the stiffness optimization process. The thickness of the ribs affect the mass distribution and would act as variables in the mass optimization.

The above method would require modeling the spar using solid elements. And alternative to this would be to use several shell or beam elements to define the spar. The thickness or cross section of these elements could then be used as variables in the optimization.

Torque Tube – Another structure that can be used to duplicate elastic properties, in the case of the single variable assumption, is the torque tube configuration shown in Figure 3 below. The advantage here is that the spars provide a differential-bending type of stiffness and the elastic center can be easily varied along the span. In the case of optimization, the shape of the spars can be adjusted (for instance with spline control points as variables) to yield the desired bending stiffness. The relative stiffness of the fore and aft spars will determine the location of the elastic axis and thus will require

individual design variables to define their shape. The connecting tubes will then make up the required torsional stiffness with their cross section acting as the design variable.

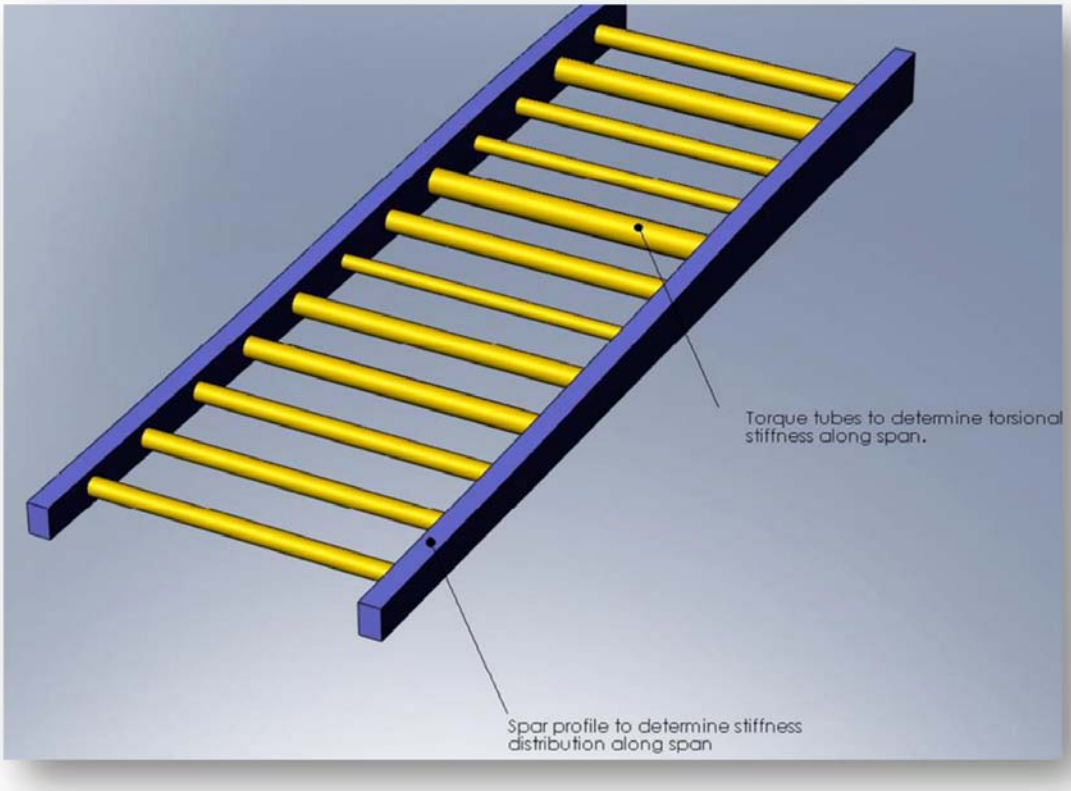

Figure 3 - Torque Tube Configuration

The torque tube structure is a simplified version of a multi-spared wing. The advantages of this configuration could be acquired with a spar/rib configuration, similar to that shown previously; if the area of the individual spar/rib connections were used as design variables (see Figure 8 below).

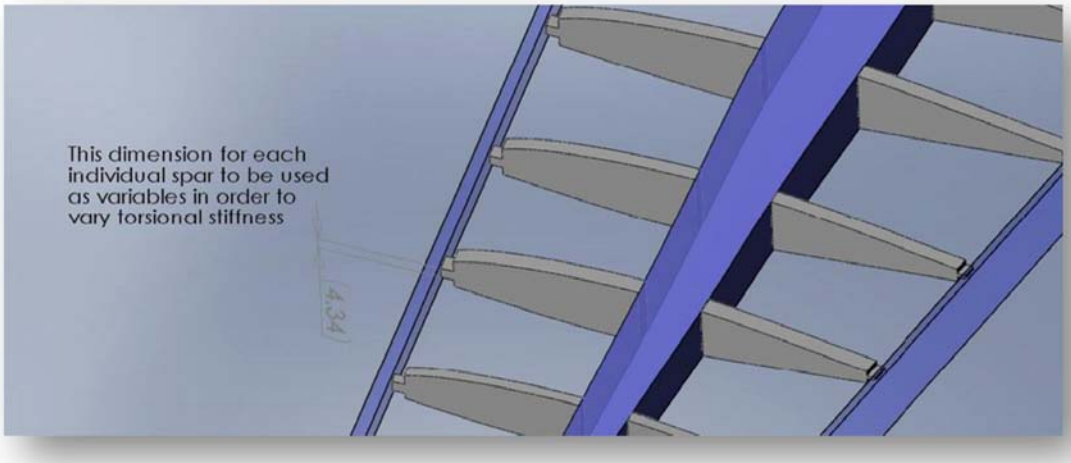

Figure 4 - Spar/Rib Configuration with Means to Match Torsional Stiffness

Internal Plate – another method for matching stiffness characteristics is through the use of an internal plate structure. In this case, the thickness of a plate is optimized to match the desired stiffness field. One option would be to use a finite element model of a plate with the thickness of each element acting as the design variables. Concentrated masses would then be placed at individual nodes and their magnitudes varied in order to match the desired mass distribution. A sensitivity analysis could quickly determine where refinement could be applied for more accurate results. An example of this is depicted in Figure 10.

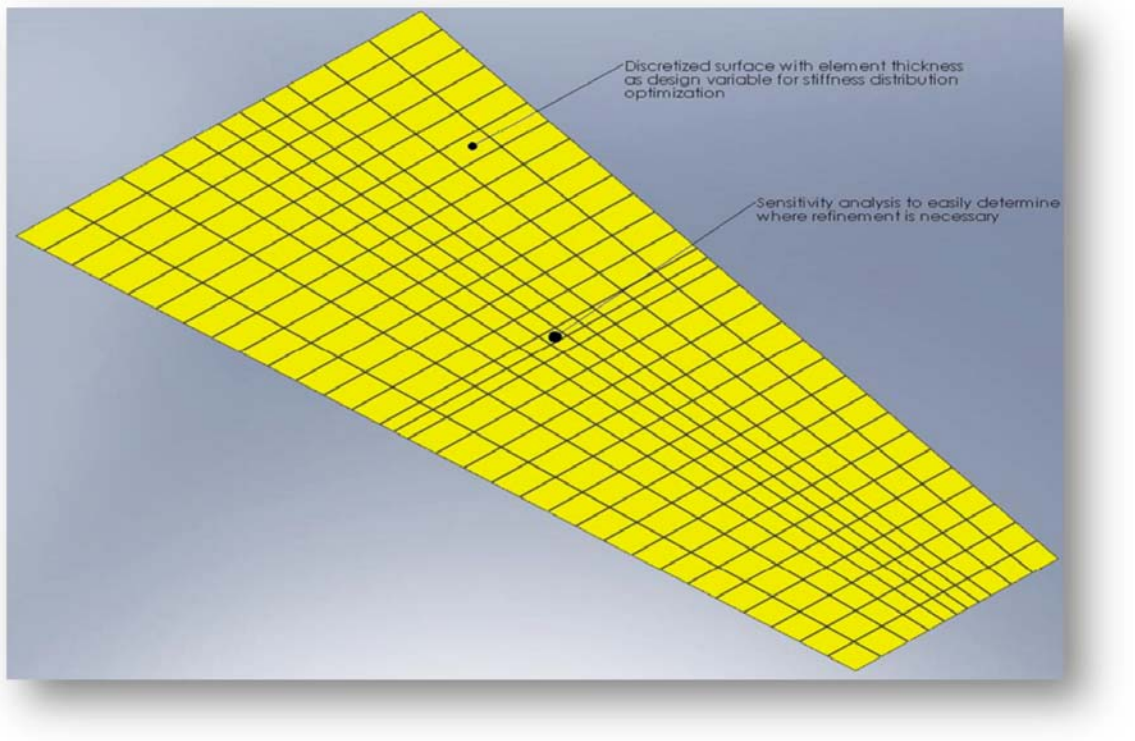

Figure 5 - Discritized Plate Model Used for Optimizing Mass/Stiffness Distribution

Another similar method could employ a contoured plate like that shown below. Here the top side of the plate is defined by a spline surface with the control point's distance (normal to bottom of plate) used as the optimization variables. This shape could then be easily machined with a CNC mill.

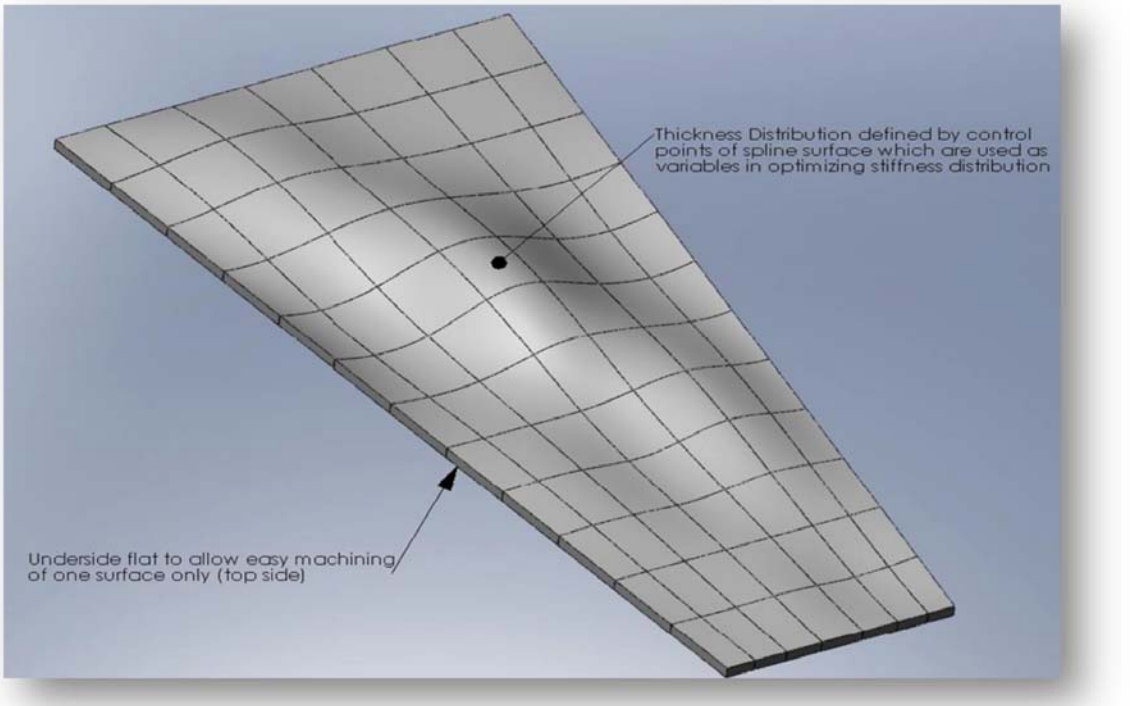

Figure 6 - Contoured Plate

Both of these plates could be used as the internal structure of the wing. The discretized model would lend itself well to a composite layup if isentropic material properties were used and the resulting plate thickness' were used to determine zones in a multi-ply composite layup.

Topology Optimization – Topology Optimization provides the capability to find an optimal distribution of material, given the design space, boundary conditions, loads, and required design performance. Using commercially available software such as MSC NASTRAN/PATRAN or Altair's Optistruct, modal frequency response can be used for the optimization inputs. The distribution of material is then optimized, subject to constraints such as bounding surfaces.

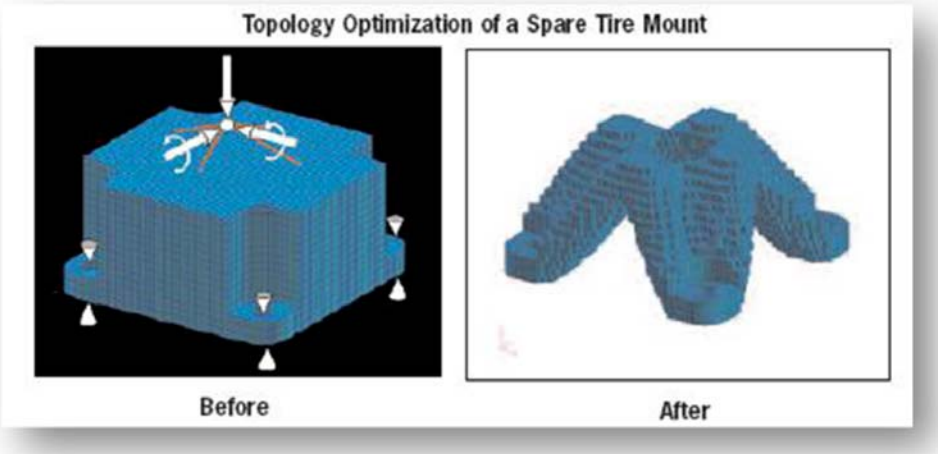

Figure 7 - Example of Topology Optimization Using Nastran

This technique has been used in aeroelastic applications such as that seen in reference (8). Figure 8 below was taken from this article and shows an optimized material distribution resulting in the desired aeroelastic response.

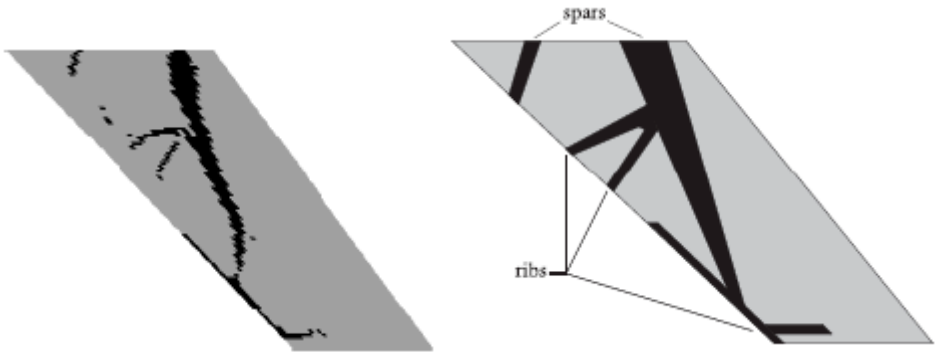

Figure 8 - Optimized Material Distribution For Given Aeroelastic Response and Practical Layout of Internal Structure

4.4.3 Issue 3 – Does Similarity Of Dynamic Response Guarantee Similar A.E. Response?

In order to determine if the assumption of a dynamically equivalent model being aeroelastically equivalent, more results should be found and compared both to the predicted full scale result as well as compared to results obtained by including aeroelasticity in the optimization loop. This could perhaps be the subject of future work.

5 Design and Aeroelastic Scaling of Boeing Joined Wing RPV

This section will highlight the methods that will be used going forward with the design of the 5m RPV. In addition, a summary of some work done to date is included here and as Appendices.

5.1 Special Consideration for Designing Flight Test Article

In addition to providing an adequate representation of the full scale aeroelastic/gust response, the flight test article must be also be designed for flightworthiness. The challenge is to balance both requirements such that the final design meets these perspectives simultaneously. The design must consider all aspects of the vehicles flight characteristics, including maneuverability and stability characteristics (during takeoff, climb, cruise, loiter and landing). Other parameters such as the vehicle weight, thrust, drag trim as well as cost must be considered.

Due to the additional requirements of the flight test vehicle, the design will proceed on two fronts. One will involve the general design of the RPV including construction methods, systems integration and defining space reservation for supporting items (such as landing gear, engines, electronics etc). This will also include the construction and testing of several preliminary models to determine flight qualities, trim requirements etc. Preliminary aeroelastic scaling work will be performed in conjunction with this. It is believed that by defining the design from both perspectives simultaneously (flight worthiness and aeroelastic response), fewer surprises will be encountered and less changes will be required later in the design process.

5.2 Methodology

Initial scaling work will be based on the assumption that a model with an equivalent dimensionless modal response to the full scale aircraft, will have the equivalent dimensionless mass and stiffness distribution. This is achieved by matching the mode shapes and dimensionless **natural frequencies** of the full scale response. Equation (17) then predicts that an equivalent model will be achieved if the remaining dimensionless aerodynamic terms are satisfied.

This assumption is beneficial in that it only requires the solution of static structural equations in the optimization routine. This then eliminates the necessity to include an aerodynamics solver, such as ZAERO, into the loop. The reduced computational cost allows a higher fidelity FE model to be used and thereby better match the mass/stiffness than would be otherwise possible.

This same assumption was used in the previous work but did not produce acceptable results throughout the test envelope. It is felt that this is due to the shortcomings addressed in section 4.3 rather than the validity of this assumption itself. Additional scaling work may be performed using other methods, such as those being used by Cooper et al, where aeroelasticity is included in the optimization loop. This can then serve to compare the methods.

5.3 Scaling Procedure

The scaling process is similar to that performed in the previous work. Gradient based optimization will be performed using commercial software such as ANSYS or NASTRAN and aeroelastic results found using ZAERO. One difference will likely include the addition of second loop in the inner optimization routine (orange area). This will allow more accurate matching of the modal response than was achieved in the previous work. For instance, one could serve to optimize the stiffness distribution (ie matching static deformations) while the other optimizes the mass distribution (ie matching mode shapes/frequencies).

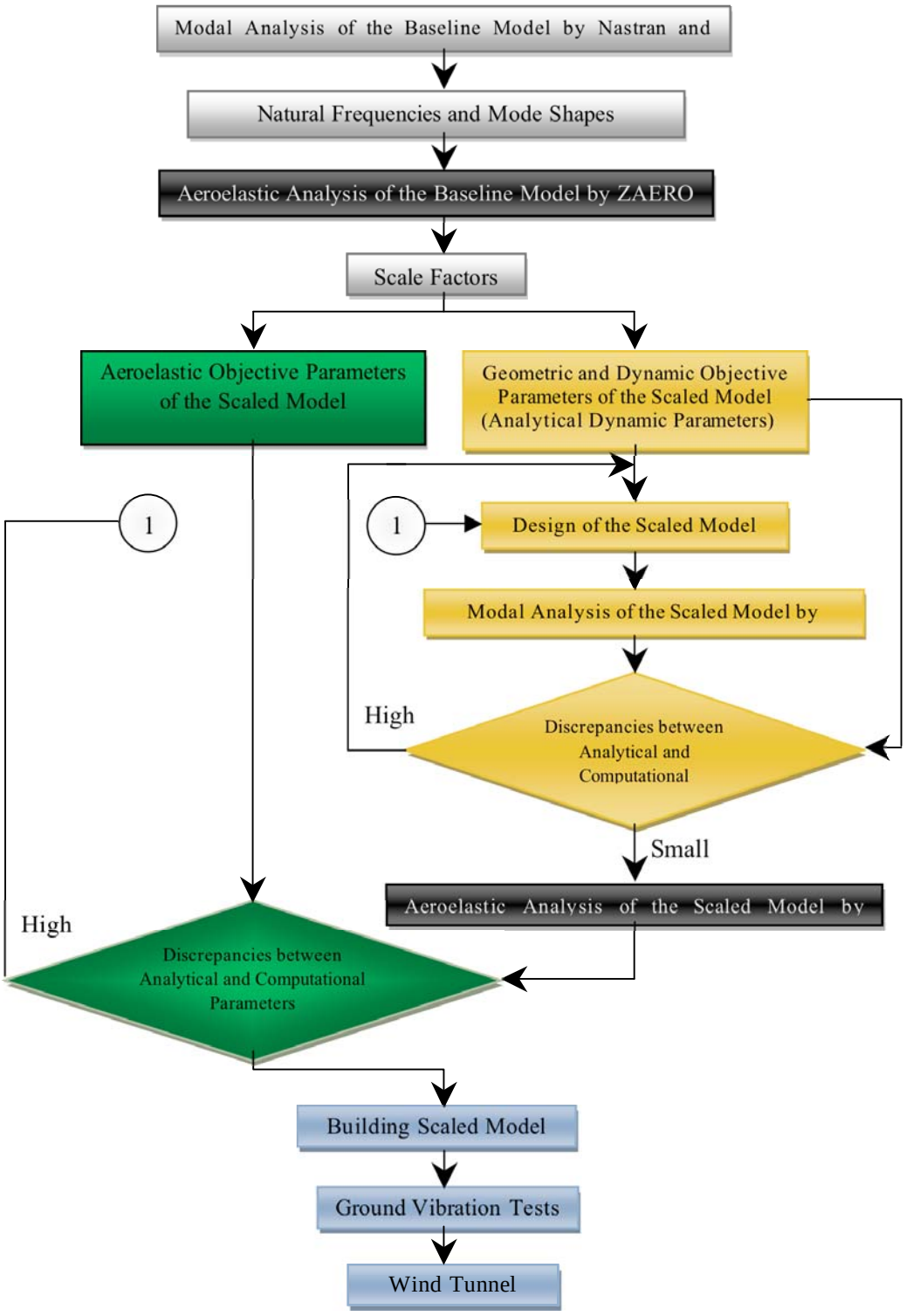

Figure 9- Proposed Scaling Method and Subsequent Validation

6 Estimate of Scaled Weight Break Out

The following section outlines the structural weight of the RPV. The values given the minimum accounting only for the structure/systems required for flight testing. The goal is to keep these weights to a minimum to allow subsequent distribution of weights in order to match the overall scaled mass, and its distribution, as determined by the aeroelastic scaling performed above.

Table 2 - Scaled Weight Breakout

	Item	Description	Weight (grams)
1	Structure	Structural members, aero envelope etc	tbd
2	Propulsion	2 x turbofan engines and supporting systems	4990
3	Landing gear	Robart Retractable Tricycle Configuration	TBD
4	Receiver	2 x for redundancy	30
5	Batteries	2 x one per receiver	100
6	Servos	7 x heavy duty	595
7	Payload/Fuel	TBD	TBD
8	Sensors/DAQ	To determine wing bending	2450
		Total Weight	TBD

Just as the weights of these individual components are important in defining a suitable model to use for the RPV, so are their physical size and shape. Considering this, any candidate designs will include space reservations for all of these components so that no design changes are required late in the design cycle.

7 Estimate of Scaled performance

A combination of Vortex Lattice methods and computational fluid dynamics is used to predict the aircraft performance. Non-dimensional stability derivatives and trim calculations are determined primarily using HASC panel code while CFX is used to compare/validate results and scope individual flight cases of particular concern. In addition, a quantitative estimation of the flight characteristics and trim states of the aircraft is being explored with the use of a 2.5 meter, remote controlled glider based on the Sensorcraft arrangement. A summary of preliminary results are included here.

7.1 Aerodynamic Prediction Using Vortex Lattice Methods

Vortex Lattice methods have been used successfully in the past to obtain aerodynamic properties of joined wing configurations. HASC (High Angle of Attack Stability and Control) code utilizes these methods and has been used in one of these previous analyses (9). For this reason, it will be used here for determining aerodynamic coefficients and stability derivatives.

The following figure shows the preliminary models analyzed in HASC. Here the surfaces representing the main wing/body, the vertical strut and the rear wings can be seen, as well as their panel distribution.

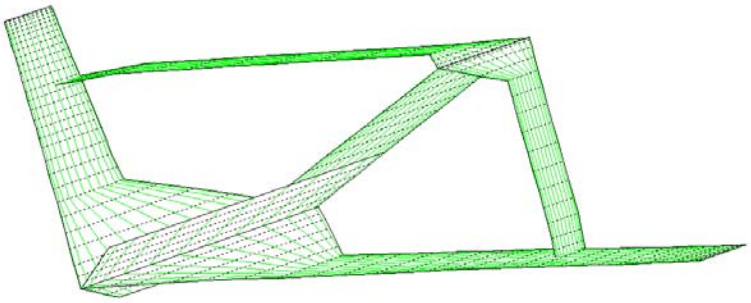

Figure 10 - Isometric View of Model

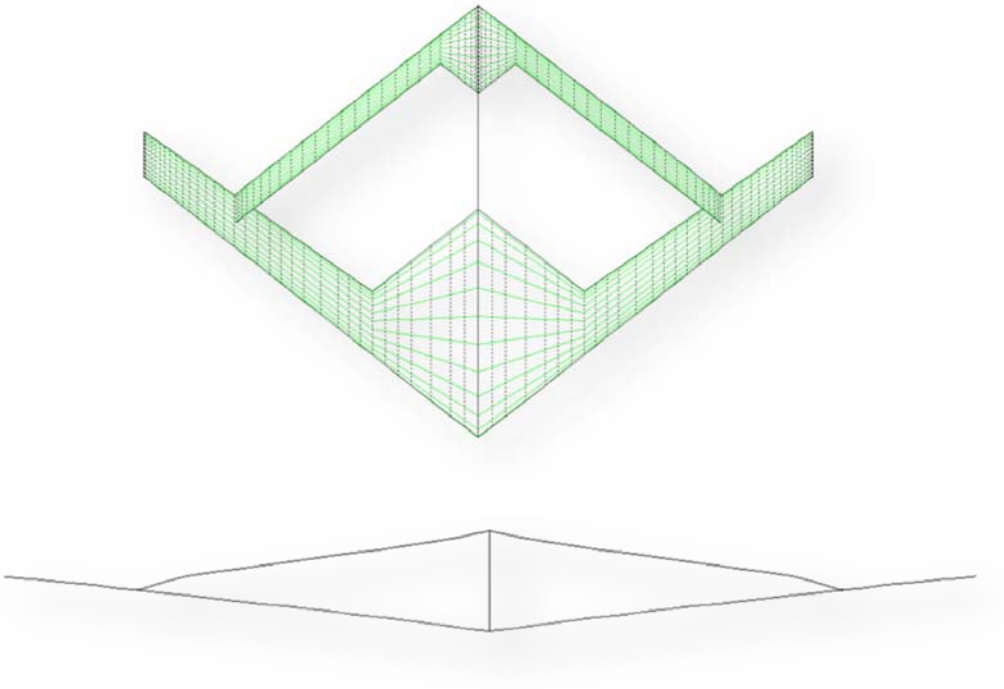

Figure 11 – Plan and Front View of Model

The above model was used to calculate a range of forces/coefficients at an array of angles and rates. These are used to calculate various stability derivatives (more information can be found in **Error! Reference source not found.** Calculation of Stability Derivatives for RPV)

Further work includes the full complement of control surfaces and a complete dynamic stability analysis. These will be used for trim analyses for both straight and level flight as well as at several bank angles. Span-wise lift distribution on all surfaces during bank will be investigated to predict stall and further improve control surface placement. Force/moment data will also yield a range of hinge moments that will be used to size control servos.

The resulting models will be compared to CFD results discussed previously as well as the wind tunnel results obtained by Bond et al (2006).

7.2 Computational Fluid Dynamics Analysis

A CFD analysis is presently being performed on the 5m geometry at no additional cost to the project. A graduate student presented availability and interest in carrying a CFD analysis of the 5m RPV and these results will be used to validate the aerodynamics of the flight vehicle. Results will be used to calculate critical stability derivatives. In addition, the CFD analysis will yield more accurate drag predictions than the Vortex Lattice Method as it will account for viscous effects. Figures 12 and 13 show an example surface mesh of the geometry and pressure contour plots of an initial analysis.

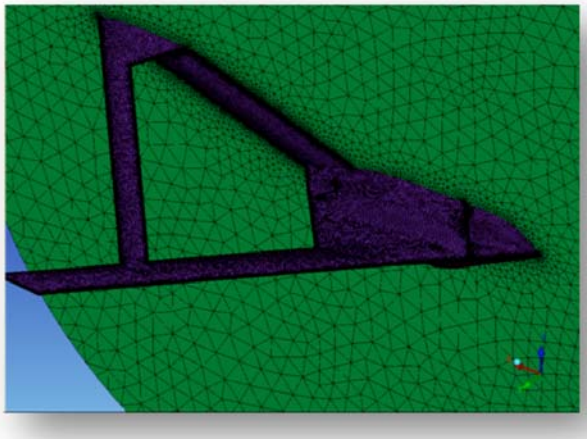

Figure 12 - Surface Mesh of RPV Generated with ICEM Software

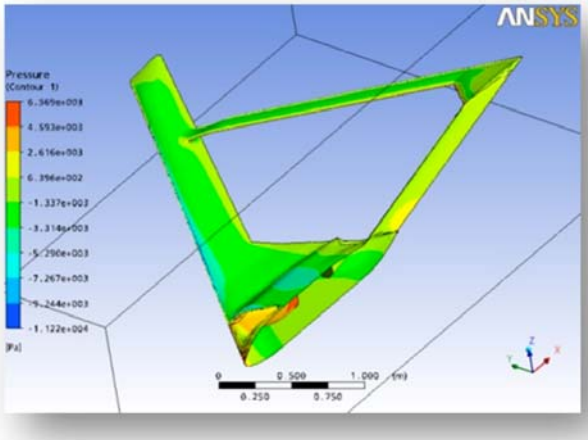

Figure 13 - Pressure Contours of Preliminary Analysis

Wind tunnel analyses were performed by Bond et al on a nominal configuration of the Sensorcraft. These will serve as a benchmark for the CFD work done here.

If sufficient agreements can be achieved for the WT and CFD results, further CFD analyses will be performed at different test points throughout the flight envelope. In addition, the validated aerodynamic model can then be used as an input to a Fluid Structure Interaction (FSI) analysis using ANSYS Multiphysics. FSI couples the aerodynamic model obtained in ANSYS CFX and the optimized structural model. The ANSYS Multi-field solver allows bidirectional FSI for analysis with deforming geometry. The computational requirements for an analysis as complex as this, will require huge amounts of computational resources and time. It would be valuable to compare the scaled results obtained using the linear small displacement assumptions and those obtained using more complex models.

7.3 Remote Controlled Glider Model

Work is underway on the construction of a 2.5 meter wingspan model of the Sensorcraft concept. It is intended to be flown in preliminary tests to determine flying qualities, trim states etc.

The model is geometrically scaled directly from the supplied CATIA geometry and is constructed using foam core with glass covering. The aircraft is unpowered and will be used as a "slope glider", using the updraft crated from the wind being deflected up by hills, cliffs etc. (this is particularly good from a gust response standpoint).

8 Sensors/Data Acquisition

A number of sensors will be employed to determine wing bending and compare to the analytic results. The wind tunnel testing of a previous joined wing model made use of sensors and data acquisition systems that may be adequate for this analysis. Table 3 outlines individual components, their weights and rough size estimates.

Table 3 - On Board Components for Determining Wing Deflection and Monitoring Telemetry

	Item	Weight (g)	Approx. Size (mm)
1	Processor Unit	782	250x100x80
2	Signal Conditioning Unit	192	100x80x50
3	Amplifier	752	200
4	Batteries	656	200x120x90
5	Other Components	100	tbd
6	Eagle Tree Systems Seagull Pro Wireless Telemetry System	120	100x100x100

The above system is limited in the number of sensor inputs as well as on-board memory. As such, several other options are being considered (see Detailed Flight Plan for more information).

9 Flight test plan

A preliminary flight test plan has been drafted and has been delivered in November 2007 (10).

10 Project Timeline and Budget

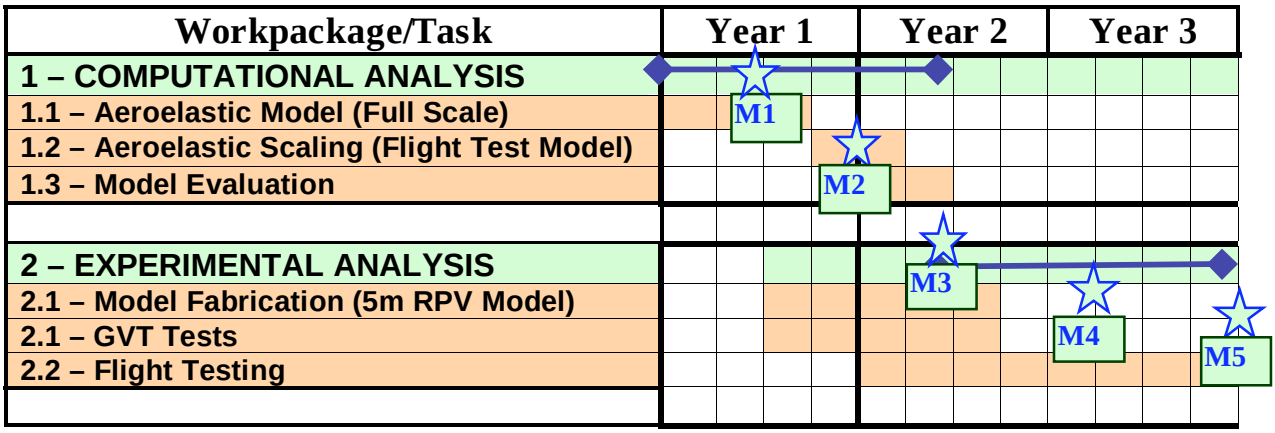

WP 1 –AEROELASTIC SCALED MODEL
(JANUARY 2008 – DECEMBER 2008 2007)

Task 1.1 – Aeroelastic Model of the full scale M1

Task 1.2 – Aeroelastic Scaling and Model Evaluation M2

Task 1.3 – Model Evaluation

WP 2 –EXPERIMENTAL ANALYSIS
(JANUARY 2009 – DECEMBER 2010)

Task 2.1 – Model Fabrication M3

Task 2.1 – GVT testing of 5m RPV model M4

Task 2.2 – Flight testing of the 5m span aereoelastic scaled Flight Vehicle M5

Cost Proposal

For Research Period 1st January 2008 to 31st December 2010

- USAF/EOARD = U.S. Air Force/European Office for Aerospace Research and Development
- IDMEC/IST = Instituto de Engenharia Mecânica

2.	Labor: (salaries, wages, etc.)	
	a. Senior Scientific Researchers (Dr Engineering) 12 hours/wk * 150 weeks at $50 per hour (3 years)	$90,000
	b. Graduate Student (Full-Time – 2 years)	**$50,000**
	c. Technician/Model Builder (3 years – part-time)	$60,000
3.	Research Facilities	
	a. Wind Tunnel testing: 50 hours x $200.00/hour	**$10,000**
	b. Machine Shop (100 hours x $100.00/hour)	**$10,000**
	c. Computational laboratory and software (3 years)	**$30,000**
4.	Expendable supplies and materials:	
	a. Prototype fabrication	$50,000
	b. Consumables	$15,000
	c. Administrative Expenses/overheads:	$10,000
	TOTAL PROJECT COST	**$325,000**
	Scholarship from FCT-Portugal (IDMEC/IST)	**$ -50,000**
	Portuguese Air Force Facilities (WT, Machine Shop and Computational)	**$ -50,000**
	EOARD/USAF requested funding	**$225,000**

The cost/year from EOARD/USAF will be USD$ 75,000/Year over a period of 3 years

11 References

1. **Pereira, P, Almeida, L. and Suleman, A.** *Aeroelastic Scaling and Optimization*. s.l. : AIAA, 2007.

2. **McClelland, William A.** *Inertia Measurement and Dynamic Stability Analysis of a Radio-Controlled Joined-Wing Aircraft.* Wright-Patterson Air Force Base : Air Force Institute of Technology, 2006. AFIT/GA/ENY/06-M07.

3. **French, Mark.** *Design of Aeroelastically Scaled Wind Tunnel Models Using Sensitivity Based*. s.l. : School of Engineering, University of Dayton, 1993.

4. **Ezequiel, Pedro.** *Aeroelastic Scaling and Optimization of a Joined-Wing Concept.* Lisboa : Universidade Téchnica De Lisboa, IST, 2007.

5. **Bisplinghoff, Raymond L, Ashley, Holt and Halfman, Robert L.** *Aeroelasticity.* Boston : Addison-Wesley Publishing Company Inc, 1957.

6. **Pittit, Chris L, Cranfield, Robert A and Ghanem, Roger.** *Stochastic Analysis of an Aeroelastic System.* New York : ASCE, 2002.

7. **Pereira, Pedro, Reis de Almeda, Luis and Costa, Antonio.** *Research and Development of a Scaled Joined-Wing Flight Vehicle*. s.l. : IDMEC/US Air Force, 2006.

8. **Hegg, Jennifer, Spain, Charles V and Rivera, J A.** *Wind Tunnel to Atmospheric Mapping Surfaces for Static Aeroelastic Scaling*. Hampton : NADA Langly Research Center.

9. **Maute, K and Allen, M.** *Conceptual Designs of Aeroelastic Structures by Topology Optimization*. s.l. : Springer-Verla, 2002.

10. **Bond, Vanessa and Maxwell, Blair.** *Free Vibration Modal Data for the Sensorcraft Boeing 410 E4-21R2*. Dayton : AFIT/USAF, 2006.

11. **Richards, Jenner G.** *Detailed Flight Test Plan, 5m Sensorcraft RPV.* Sintra : Portuguese Air Force Academy, 2007.

12. **Cooper, Professor J E, et al.** *Experimental Validation of an Aeroelastic Scaled Sensorcraft Model.* 14th November 2007. EOARD Contract FA 8655-07-1-3111.

Appendix A - **Calculation of Stability Derivatives for RPV**

Work has begun in exploring the flightworthiness of the test article and includes a static/dynamic analysis of the RPV using vortex lattice methods. HASC (High Angle of Attack Stability and Control) software is used for the analysis of the aerodynamic coefficients and stability derivatives. Reference (1) is used as a guideline for the process with several additional items investigated here.

The code is comprised of three routines; VORLAX, VTXCHN and VORLIF. Of the three, only VORLAX is used in this analysis (the vortex lattice routine). VORLIF and VTXCHN are used to account for vortex shedding (and resulting breakdown) from wing strakes and chinned fore-bodies. These effects were not required for consideration in the last analysis and therefore will not be used here either. These phenomena are most prevalent in the case at very high angles of attack and with geometry such as low aspect and delta wings, strakes or canards and chined fuselages.

The figure below shows the HASC model used for the analysis (MATLAB was used to visualize panel geometry). The model accounts for the lifting surfaces as well as the vertical projection of the fuselage onto the xy plane. Airfoil camber is obtained from the supplied CAD geometry at 13 different stations and applied to both the lifting and control surfaces. The stability derivatives with respect to the off wind angles are summarized in Table 4 below and those due to the control surface deflections are given in Table 5 (note: these are preliminary results and do not reflect updated mass properties and cg locations).

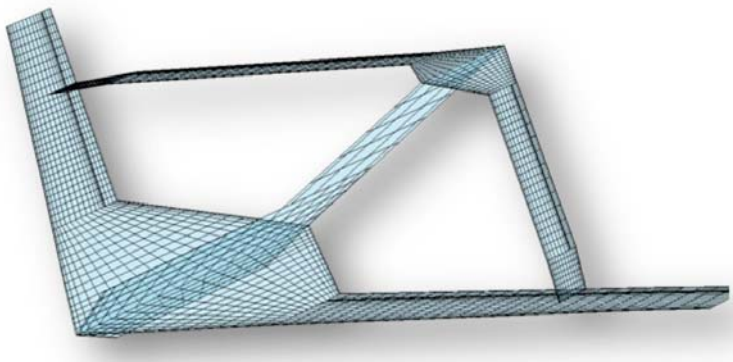

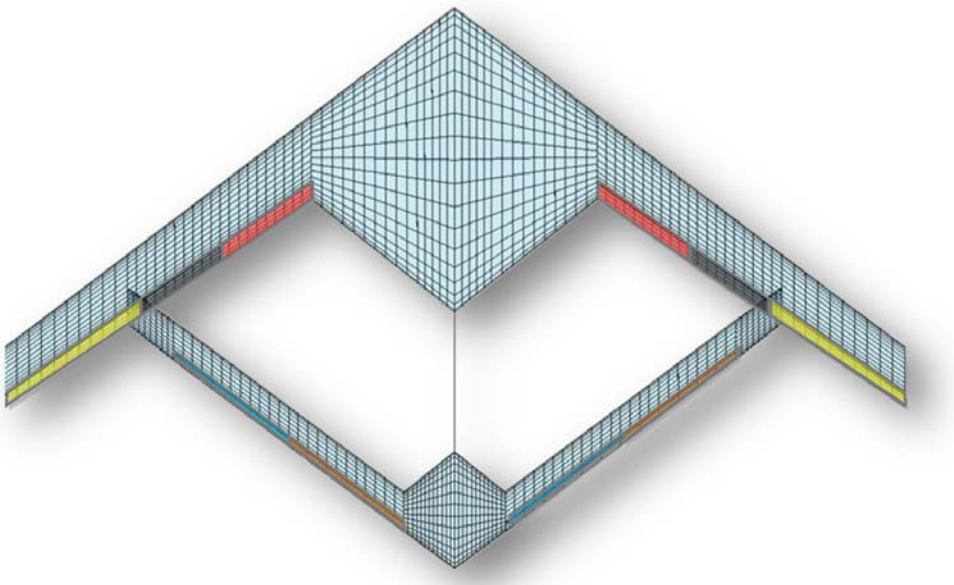

Figure 14 - HASC Model with Control Surfaces

Table 4 - Stability Derivatives for Off Wind Conditions

Alpha Derivatives		Beta Derivatives		Roll Derivatives		Pitch Derivatives		Yaw Derivatives	
CLa	11.076	CLb	0.000	CLp	0.000	CLq	55.406	CLr	0.0000
CYa	0.000	CYb	-0.568	CYp	0.266	CYq	0.000	CYr	0.3411
Cla	0.000	Clb	-0.363	Clp	-0.948	Clq	0.000	Clr	0.3612
Cma	-14.094	Cmb	0.000	Cmp	0.000	Cmq	-144.959	Cmr	0.0000
Cna	0.000	Cnb	0.096	Cnp	-0.169	Cnq	0.000	Cnr	-0.0823

Table 5 - Stability Derivatives With Respect to Control Surface Deflections

δ_{Flaps}		$\delta_{inner\ Aileron}$		$\delta_{Outer\ Aileron}$		$\delta_{inner\ Elevator}$		$\delta_{Outer\ Elevator}$	
CLa	1.60E-02	CLb	5.65E-03	CLp	0.00E+00	CLq	9.20E-03	CLr	9.02E-03
CYa	0.00E+00	CYb	-3.38E-03	CYp	-2.73E-04	CYq	0.00E+00	CYr	0.00E+00
Cla	0.00E+00	Clb	-4.03E-03	Clp	-1.92E-03	Clq	0.00E+00	Clr	0.00E+00
Cma	-5.09E-03	Cmb	-6.65E-03	Cmp	0.00E+00	Cmq	-4.29E-02	Cmr	-3.23E-02
Cna	0.00E+00	Cnb	7.53E-04	Cnp	-2.60E-05	Cnq	0.00E+00	Cnr	0.00E+00

From the calculated stability derivatives a dynamic analysis was performed to determine the flight qualities. Initial results show good stability characteristics in all modes besides Dutch roll (the aircraft shows marginal instability in this mode[2]).

From the VLM results additional information is processed, including trim states at various flight conditions, spanwise loading at these trim states (avoid tip stall in banking maneuvers) and hinge moments (to aid in servo sizing).

Work is also underway on the construction of a 2.5 meter wingspan model of the Sensorcraft concept. It is intended to be flown in preliminary tests to determine flying qualities, trim states etc. The model is geometrically scaled directly from the supplied CAD geometry and is constructed using foam core with glass covering. The aircraft is unpowered and will be used as a "slope glider", using the updraft crated from the wind being deflected up by hills, cliffs etc. (this is particularly good from a gust response standpoint). Figure 15 below shows the foam core that was used for the fuselage of the glider.

[2] *It should be noted that the cg locations and the scaled mass were not known at the time of this analysis. The above results are only included as a proof of the method. However, the process has been automated using using tools such as Matlab and the final calculations are now underway using the recently supplied data.*

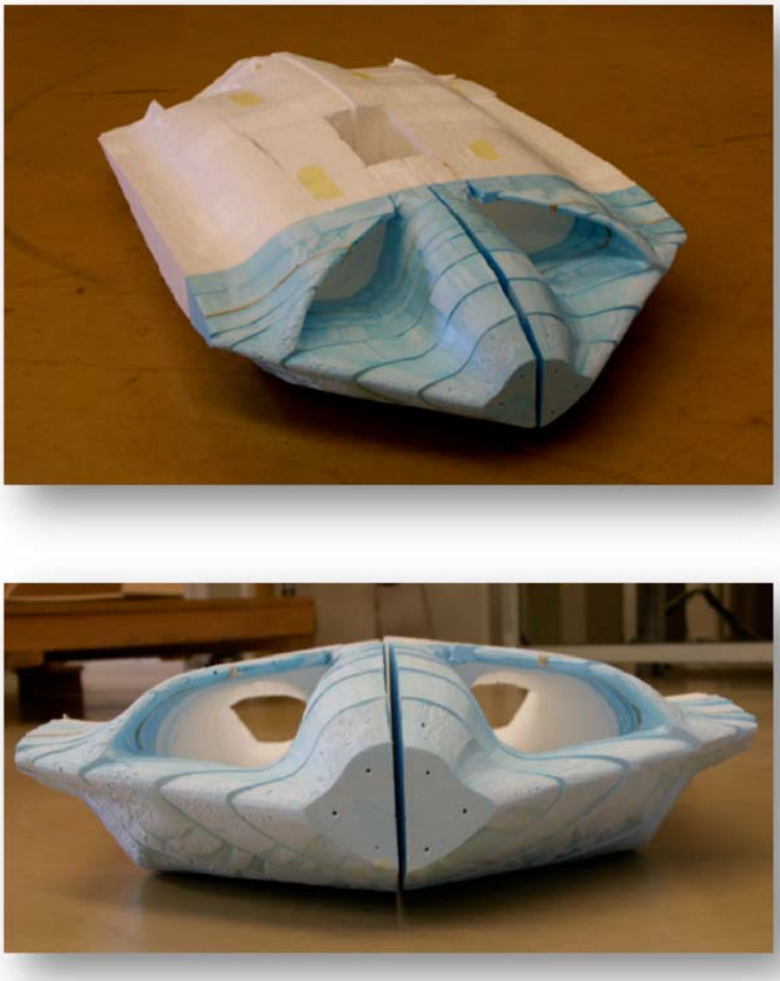

Figure 15 - Foam Plug for 2.5m Glider Fuselage

Additional Work

Additional work is being conducted in areas such as specifying the aircraft components, supporting systems etc. In addition, the flight test plan has been drawn up and is being amended as more information becomes available. A drag model is being determined using CFD and classical empirical methods which will be used to update the dynamic analysis, spec engines etc.

The HASC calculations coefficients and derivatives were compared to results using AVL 2.6 vortex lattice method to increase confidence in results. All data showed good agreement and served to validate the use of AVL for this model. AVL will be used for several calculations including estimation of form drag (interpolates drag polars at local C_l for each airfoil section) and to query loading distributions along the span.

Final calculations are being performed at present in order to complete the stability analysis. There is some discussion as to the scaled flight condition to be used, in addition to the control scheduling intended by Boeing. Once these have been determined the results will be completed and summarized in an upcoming document.

These results will include the following:

- Trimmed aircraft states for several critical flight conditions
- Spanwise loading for several trimmed banked conditions to insure acceptable stall characteristics (ie no tip stall)
- Hinge moments for control surfaces to be used for servo sizing
- Lateral and longitudinal dynamic stability analysis at several critical trimmed states.